

Synthesis and characterisation of a new organic-inorganic hybrid compound (NH₄)₂(2A4MPy)₆(H₂V₁₀O₂₈)·H₂O

Tawel Oumrou Taleb Amar¹, Ahlem Maalaouia¹, Aliou Hamady Barry², Aride Jilali³,
Samah Akriche*¹

1. Laboratoire de Chimie des Matériaux LRI3ES08, Faculté des Sciences de Bizerte Université de Carthage, 7021 Zarzouna, Bizerte, Tunisia.
2. Laboratoire de Chimie des Matériaux, Faculté des Sciences et techniques, Université de Nouakchott Al Aasriya (UNA) - Nouakchott – Mauritanie.
3. Mohammed V University in Rabat, Centre Sciences des Matériaux, Laboratoire de PhysicoChimie des Matériaux Inorganiques et Organiques (LPCMIO), Ecole Normale Supérieure (E.N.S), Rabat, Morocco.

Infos

Received: 15 February 2022
Accepted: 09 August 2022

Keywords - Mots clés

Decavanadate; Synthesis; Single-crystal XRD; thermal analysis

Corresponding authors emails:

tawel.talebamar@gmail.com

Abstract - Résumé

A new organic inorganic decavanadate, [NH₄]₂[2A4MPy]₆[H₂V₁₀O₂₈]₂·H₂O (2A4MPyV10), crystal was synthesized by slow evaporation and characterized. It was by means of single crystal X-ray diffraction, IR spectroscopy and thermal analysis. Its crystal structure revealed that it crystallizes in the orthorhombic system with non-centrosymmetric space group *Fdd2* with *a* = 17.6311(5) Å, *b* = 22.6421(9) Å, *c* = 38.8032(9) Å, *V* = 15490.4(8) Å³. The X-ray structure determination revealed the presence of deprotonated decavanadate cage-like clusters [H₂V₁₀O₂₈]⁴⁻ (V10) bridged via strong O_{decavanadate}—H...O_{decavanadate} hydrogen bonds to generate ribbons extending along the *a*-axis. Whereas the lattice water molecule and the organic moieties are associated to the polymeric species by multiple hydrogen bonds (N—H...O, N—H...N, O—H...O) and reside between the inorganic ribbons giving rise to 3D supramolecular network.

1. INTRODUCTION

Polyoxovanadate (POVs) are obtained via the self-aggregation of mononuclear vanadium-oxo ligands giving rise to novel species with fascinating structural diversity. In recent years, polyoxovanadate clusters have aroused major interest because these molecular fragments encapsulate charged or neutral species that function as structural directors in the self-organization process of the formation of the metal oxide cage [1-6]. They can also be good model systems in the design of complex materials intermediate between molecular compounds and infinite solids [7-10]. Organic-inorganic polyoxovanadates hybrid materials combine the advantageous characteristics of both organic and inorganic components [8-9]. Among them, the most important subclass of decavanadate, are extensively studied because of their potential physical and therapeutic applications[10]such as medicinal agents for diabetes [11] and as an excellent candidate antineoplastic antitumor agent against human cancer [12], tuberculosis and anemia[13] etc. Additionally, the prominent subclass of POVs, the decavanadate based materials are also widely used as potent inhibitor of adenylate kinase, hexokinase, and phosphofructokinase [14-17] and even for their effective inhibition towards both actin and ATP of the actin-stimulated myosin-ATPase activity [17]. Decavanadate hybrids are attracting increased attention of materials chemists for their structural phase transitions, electrical, magnetic and optical properties [18-19].

The synthesis of new decavanadate species is mainly depended to several experimental conditions such as controlling the pH, mole ratio, the temperature, counter ion, etc. The inorganic and/or organic counter ions play a major role as well as the other factors for directing the crystalline network of POVs materials. Herein, we have successfully synthesised a new compound of the formula $[\text{NH}_4]_2[\text{2A4MPy}]_6[\text{H}_2\text{V}_{10}\text{O}_{28}]_2 \cdot \text{H}_2\text{O}$ (2A4MPy = 2-amino-4-methylpyridinium). Its crystal structure, spectroscopic and thermal properties are reported.

2. EXPERIMENTAL

2.1. Materials and instrumentation

All reagents for syntheses were purchased from commercial sources and used as received without further purification. Elemental analyses (C, H and N) were performed on a Perkin-Elmer 2400 CHN Elemental Analyzer, and that of V were analyzed on a Plasma-spec (I) ICP atomic emission spectrometer. The IR spectrum was recorded in the range of $4000\text{--}400\text{ cm}^{-1}$ on an Alpha Centaur FT/IR spectrophotometer using KBr pellets. TG-DTA92thermoanalyzer was used to perform thermal treatment. The TG thermogram was obtained with powder samples placed in an open platinum crucible and heated in air from room temperature to 500°C with $5^\circ\text{C}/\text{min}$ heating rate.

2.2 X-ray diffraction

The crystal structure was determined from the single crystal X-ray diffraction data obtained with a Nonius Kappa CCD and CAD4 Enraf Nonius diffractometers (Graphite monochromated, $\text{MoK}\alpha = 0.71073$). The structure was solved by direct method using the program SHELXS-97 [14] and refined on F^2 by full matrix least squares method using SHELXL-97 [20] in the WINGX [21]. All non-hydrogen atoms were refined isotropically and then an isotropically. Hydrogen atoms of organic moiety were placed geometrically and treated as riding in geometrically optimized positions. Ammonium, water and decavanadate H atoms were refined using restraints [$\text{X-H} = 0.85$ (2) Å, (X : N/O) and $\text{Uiso}(\text{H}) = 1.5 \text{ Ueq}(\text{X})$]. Crystal data and structure refinement are summarized in Table 1. The selected bond lengths and angles are listed in Table S1.

2.3. Synthesis

A mixture of sodium metavanadate NaVO_3 (0.09 g, 10 mmol), and 2A4MPy (0.042 g, 6 mmol) was dissolved in 30 mL of distilled water at room temperature. The mixture was stirred for 1 h until it was homogeneous. Then the pH value of the mixture was adjusted to about 5 with 3 M hydrochloric acid. After

Table 1: Crystallographic data and structure refinement parameters for 2A4MPyV10.

Formula	$\text{C}_{36}\text{H}_{68}\text{N}_{14}\text{O}_{57}\text{V}_{20}$
FW	1492.18
Crystal system	Orthorhombic
Space group	$Fdd2$
a (Å); b (Å); c (Å)	17.6311 (5); 22.6421 (9); 38.8032 (9)
α (°) = β (°) = γ (°)	90
V (Å ³)	15490.4 (8)
Dx (Mg m^{-3})	2.254
Crystal size (mm)	$0.15 \times 0.11 \times 0.09$
$F(000)$	10384
Absorption coefficient (mm^{-1})	2.23
Radiation (Å)	$\lambda = 0.71073$
Theta min–max (°)	2–34.5
Index ranges	$-22 / h / 22$; $-28 / k / 28$; $-49 / l / 49$
Observed data [$I > 2.0 \sigma(I)$]	5610
Reflections independant	7235 ($R_{\text{int}} = 0.028$)
R_{int} , $wR(F)$, S	0.080, 0.076, 1.02
Minimum and maximum resd. dens. ($\text{e}/\text{Å}^3$)	-0.72 ; 0.71

removal of the precipitate by filtration, the clear solution was allowed to evaporate in the air at room temperature. Seven days later, some yellow block crystals were obtained adequate for X-ray crystallography analysis. Chemical analysis for $C_{36}H_{58}N_{12}O_{32}V_{10}$: Theoretical: C: 30.50, H: 3.19, N: 5.61, V: 28.95; Experimental: C: 31.55, H: 4.09, N: 4.42, V: 27.78%.

3. RESULTS AND DISCUSSION

3.1. X-ray Diffraction analysis of 2A4MPyV10

Single crystal XRD analysis of the as-synthesised compound showed that the asymmetric unit of the crystal structure comprises of a complete decavanadate cluster anion, $[H_2V_{10}O_{28}]^{4-}$ (V10), three 2-amino-4-methylpyridinium cations, one ammonium NH_4^+ and one water molecule (Figure 1(a)).

The decavanadate polyoxoanion has a cage-like structure consisting of ten vanadium atoms and 28 oxygen atoms arranged in closed aggregates of VO_6 octahedra sharing edges, as shown in Figure 1(b). The bond valence sum calculations for the V10 ion according to Brown [22] indicate that the vanadium atoms have +V an oxidation state (V1: 5.2745 v.u.; V2: 5.3231v.u.; V3: 5.4519v.u.; V4 : 5.3310v.u.; and V5: 5.2499v.u.) in agreement with the expected $[H_2V_{10}^{+V}O_{28}]^{4-}$ subunit and thus conform with the charge balance consideration; $[NH_4]_2[2A4MPy]_6[H_2V_{10}O_{28}]_2 \cdot H_2O$. The distortion index values [23] for the VO_6 octahedra ($ID(V1O_6) = 0,43296$; $ID(V2O_6) = 0,4115$; $ID(V3O_6) = 0,25356$; $ID(V4O_6) = 0,3896$; $ID(V5O_6) = 0,43884$), are relatively high indicating a distorted octahedral geometry around vanadium atoms due to repulsions between the close-packed terminal and bridging oxygen atoms within the coordination sphere [24]. The oxygen atoms acting as ligands to vanadium central atoms can be divided into four different types: (i) eight $O_{terminal}$ ligands related to one vanadium atom, (ii) eighteen $\mu_2-O_{bridging}$ and $\mu_3-O_{bridging}$ ligands linked to two and three vanadium atoms, respectively (iii) two $\mu_6-O_{bridging}$ ligands attached to six vanadium atoms. The geometrical features of decavanadate polyanion are quite similar to those found in previously reported structures of decavanadate salts [25-30].

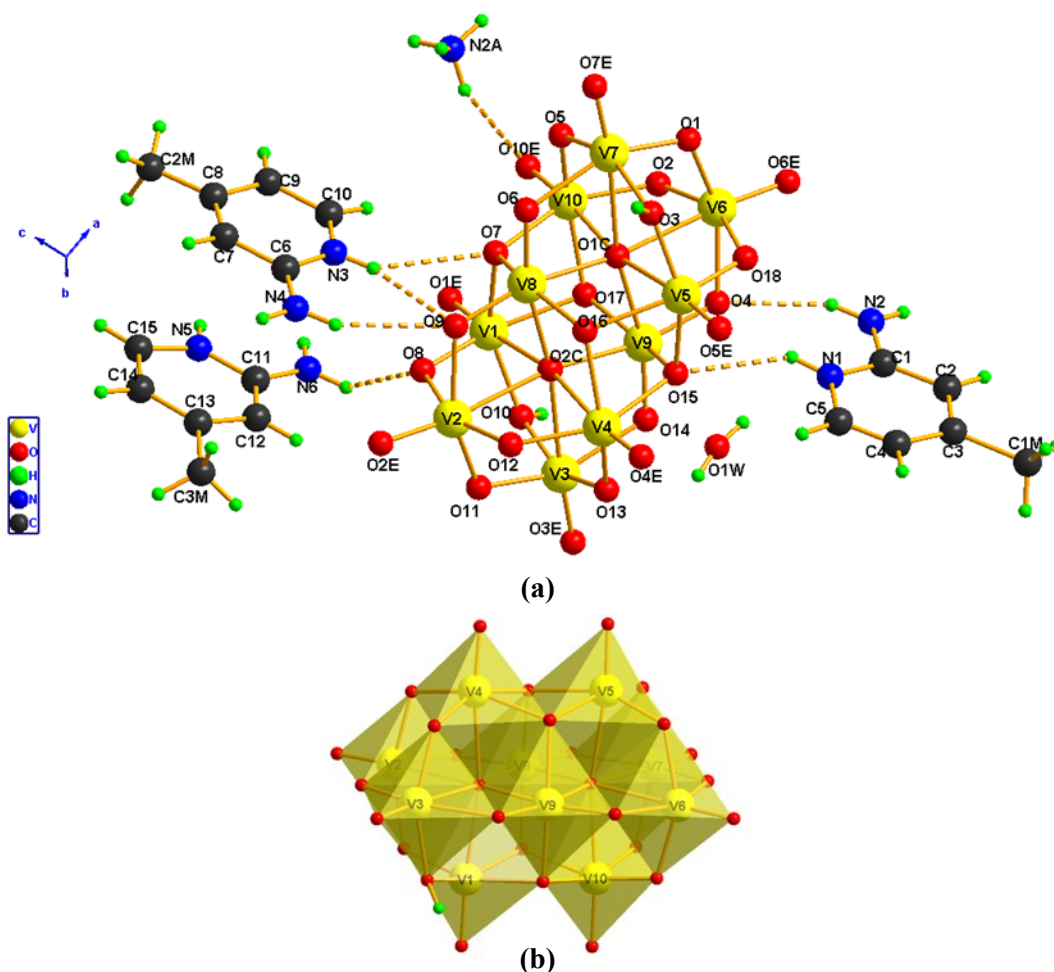


Fig. 1(a) View of structural unit of 2A4MPyV10 with the atomic numbering scheme; Hydrogen bond shown as a dotted line. (b) Polyhedral view of the decavanadate V10 cluster showing the $\{VO_6\}$ units.

An examination of the structural network of the entitled compound clearly shows a 3D supramolecular topology of decavanadate clusters interconnected with lattice water molecules and organic cations via intricate O—H...O, N—H...O, N—H...N and C—H...O hydrogen bonding patterns which seem to be the most important forces to generate this 3D supramolecular architecture and stabilize the structure, as it is illustrated in figure 2 (Table 2).

It should be noted that the deprotonated dicavanadate clusters are associated to each other through the strong $O_{\text{decavanadate}}\text{—H}\dots O_{\text{decavanadate}}$ ($O\cdots O$ distance: 2.860 (16) and 2.878 (15) Å) (Table 2) interactions giving rise to dicavanadate ribbons along the a-axis which are subsisted at $z=0$, $z=1/4$, $z=1/2$ and $z=3/4$. Both NH_4^+ and $[\text{2A4MPy—H}]^+$ cations, which are counter-ions of the $[\text{H}_2\text{V}_{10}\text{O}_{28}]^{4-}$ anions, are located between this ribbons and bridged with polyanions by a set of N—H...O, N—H...N and C—H...O interactions ($\text{N}\dots\text{O}$: 2.771 (18)-2.970(2), $\text{N}\dots\text{N}$: 2.970(2)-2.980(2) and $\text{C}\dots\text{O}$: 3.14 (2)-3.43(2)) to generate a 3D encapsulated framework.

As shown in figure 3, when the organic moieties are omitted, we can obviously observed that the water molecules reside also between the ribbons and assure the link between this chains of diprotonated decavanadate clusters via $\text{OW—H}\dots O_{\text{decavanadate}}$ giving so more stability to the supramolecular network.

For the organic cations, the two crystallographic independent cations $[(\text{C}_6\text{H}_6\text{NH}_2)\text{-N}(3)\text{H}]^+$ and $[(\text{C}_6\text{H}_6\text{NH}_2)\text{-N}(5)\text{H}]^+$ are connected through $\pi\dots\pi$ stacking interactions with a distance of separation between range in 3.735 to 3.934 Å whereas the remaining crystallographic independent cation $[(\text{C}_6\text{H}_6\text{NH}_2)\text{-N}(1)\text{H}]^+$, is associated with its symmetrical one with distance separation centroids equal to 3.933 Å as shown in figure 4.

3.2 IR spectroscopy

The infrared spectrum of 2A4MPyV10 depicted in figure 5, exhibits several medium and strong bands clearly evidenced the presence of polymeric vanadates [31-34]. In fact, the spectrum shows particular IR bands in the metal-oxygen extending region from 400 to 1000 cm^{-1} which demonstrate that the compound has the fundamental construction of decavanadate. The most noticeable band in the infrared spectrum of 2A4MPyV10 in the 1000-900 cm^{-1} region at 956 cm^{-1} is typical for the $\nu(\text{V}=\text{O})$ of the decavanadate polyanion V10 and those found at 840 and 734 and around 564 cm^{-1} are attributed respectively to symmetric and asymmetric stretching modes of the bridging V-O-V bonds. It's to be noted the specific band at about 630 cm^{-1} characteristics of protonated decavanadate anions assigned to V—Ob—H bonds according to Wery et al and Roman et al [35–36]. The spectrum clearly gives the characteristic bands of the

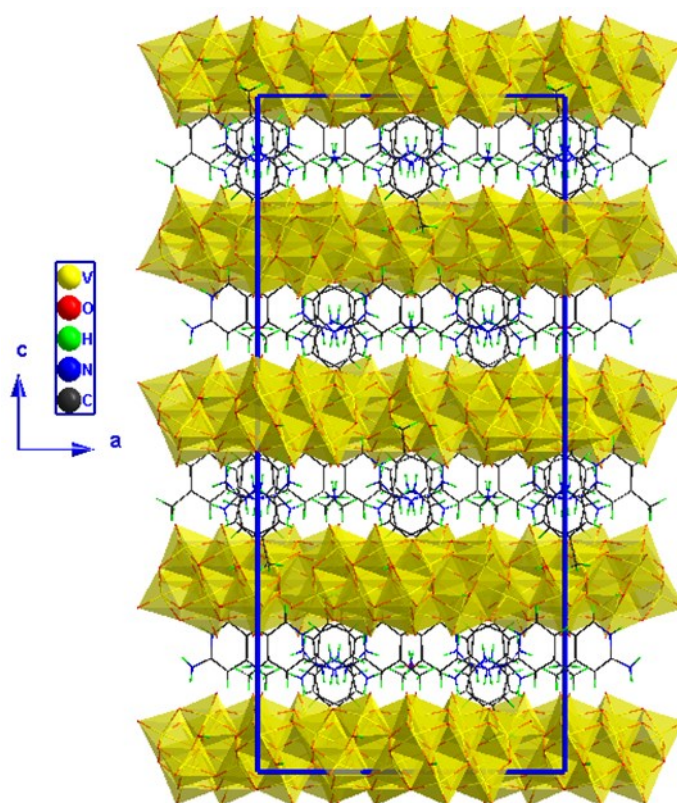


Fig.2 : View of inorganic framework along the a-axis.

Table 2 :Hydrogen-bond geometry (Å, °)

$D-H\cdots A$	$D-H$	$H\cdots A$	$D\cdots A$	$D-H\cdots A$
O10—H10O \cdots O2ii	0.90 (3)	1.99 (4)	2.878 (15)	168 (5)
N1—H1 \cdots O4	0.86	2.15	2.949 (18)	155
N1—H1 \cdots O15	0.86	2.53	3.182 (18)	134
N1—H1 \cdots O18	0.86	2.50	3.09 (2)	126
N2—H2B \cdots N2Aiii	0.86	2.11	2.97 (2)	176
N2—H2A \cdots O4	0.86	2.39	3.14 (2)	146
N2—H2A \cdots O14ii	0.86	2.18	2.817 (19)	130
C2—H2 \cdots O7Eiii	0.93	2.58	3.43 (2)	151
C4—H4 \cdots O2iv	0.93	2.48	3.39 (2)	165
N3—H3 \cdots O9	0.86	2.22	3.047 (15)	162
N4—H4A \cdots O6i	0.86	2.29	2.947 (17)	134
N4—H4A \cdots O9	0.86	2.51	3.245 (19)	144
N4—H4B \cdots N2Ai	0.86	2.12	2.98 (2)	174
C9—H9 \cdots O12v	0.93	2.40	3.31 (2)	166
N5—H5A \cdots O18vi	0.86	1.91	2.724 (14)	157
N6—H6A \cdots O5Evi	0.86	2.52	3.278 (18)	147
N6—H6A \cdots O18vi	0.86	2.37	3.060 (18)	138
N6—H6B \cdots O8	0.86	2.27	2.922 (19)	133
C12—H12 \cdots O2E	0.93	2.47	3.246 (16)	141
C14—H14 \cdots O3Evii	0.93	2.63	3.192 (19)	120
C14—H14 \cdots O6Eviii	0.93	2.22	3.14 (2)	167
O1W—H1W1 \cdots O1Eix	0.75 (4)	2.19 (6)	2.830 (15)	143 (5)
O1W—H1W1 \cdots O5E	0.75 (4)	2.33 (4)	2.840 (14)	126 (6)
N2A—H1A2 \cdots O5	0.90 (2)	2.12 (8)	2.771 (18)	129 (7)
N2A—H2A2 \cdots O13v	0.90 (2)	1.93 (3)	2.826 (19)	171 (9)
N2A—H3A2 \cdots N2x	0.86 (2)	2.30 (6)	2.97 (2)	135 (7)
N2A—H4A2 \cdots N4i	0.83 (2)	2.31 (5)	2.98 (2)	138 (6)

Symmetry codes: (i) $-x+1, -y, z$; (ii) $-x+3/2, -y+1/2, z$; (iii) $-x+7/4, y+1/4, z-1/4$; (iv) $x-1/4, -y+1/4, z-1/4$; (v) $x+1/4, -y+1/4, z+1/4$; (vi) $-x+5/4, y+1/4, z+1/4$; (vii) $-x+3/4, y-1/4, z+1/4$; (viii) $x-3/4, -y+1/4, z+1/4$; (ix) $-x+5/4, y-1/4, z-1/4$; (x) $-x+7/4, y-1/4, z+1/4$.

2A4MPy cation. The large bands observed in 3400-2800 cm^{-1} region, are attributed to $\nu(\text{OH}_2)$, $\nu(\text{NH}^+)$, $\nu(\text{NH}_2)$ and $\nu(\text{C}-\text{H})$ while the modes $\nu(\text{N}-\text{H})$; $\nu(\text{C}-\text{C})$ and $\nu(\text{C}-\text{N})$ are observed in the range 1700-1100 cm^{-1} [25]. The deformation band of water molecule occurs at 1623 cm^{-1} [37].

3.3. ATD-TG analysis of 2A4MPyV10

The differential thermal and thermogravimetric analyses of the mixed salt 2A4MPyV10 were performed with 14.2 mg of the samples, placed in a platinum crucible and heated at the rate of $5^\circ\text{C}\cdot\text{min}^{-1}$, in a wide temperature range (40 - 500 $^\circ\text{C}$) under an argon atmosphere. The two thermal curves are reported in figure 6. The first endothermic peak between 50 to 110 $^\circ\text{C}$ is attributed to the dehydration of the mixed salt, accompanied by a mass loss of about 2.04 % observed on the TG curve corresponding well to the

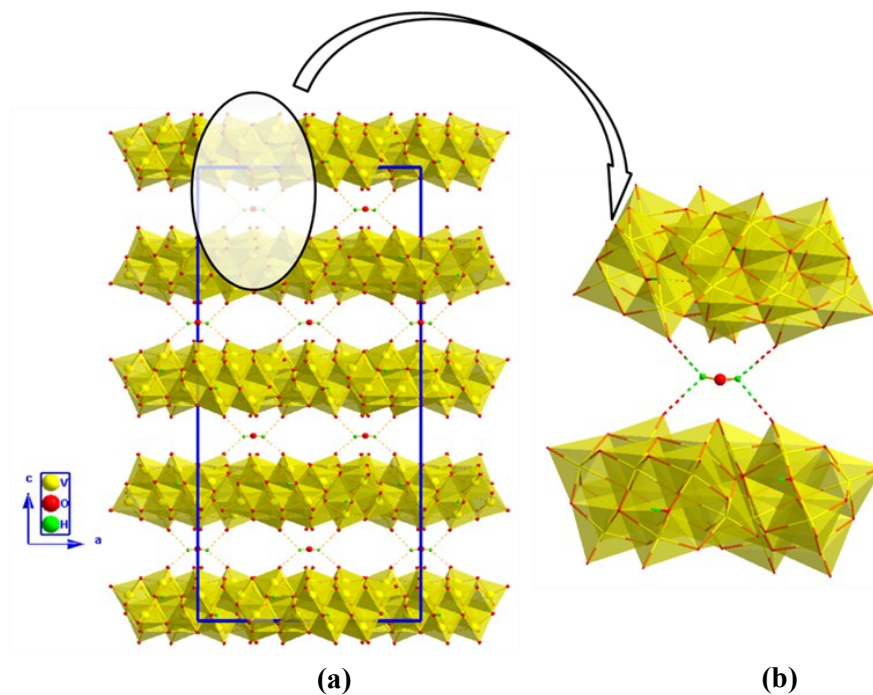


Fig. 3:(a) View of inorganic framework along the a-axis. (b)View showing the association water molecule and the V10 polyanions.

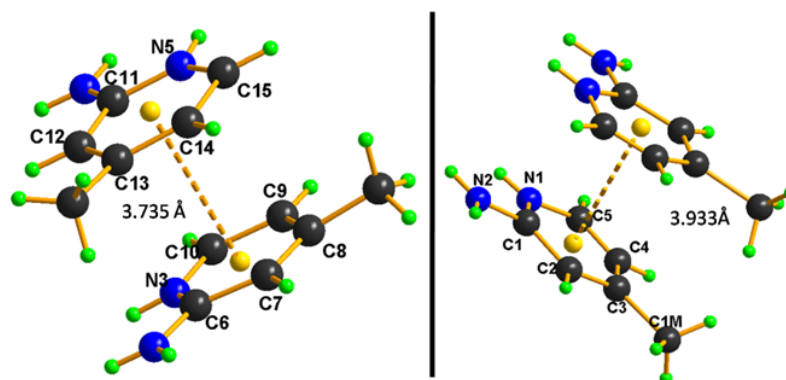


Fig.4 :stacking π ... π interactions between organic moieties.

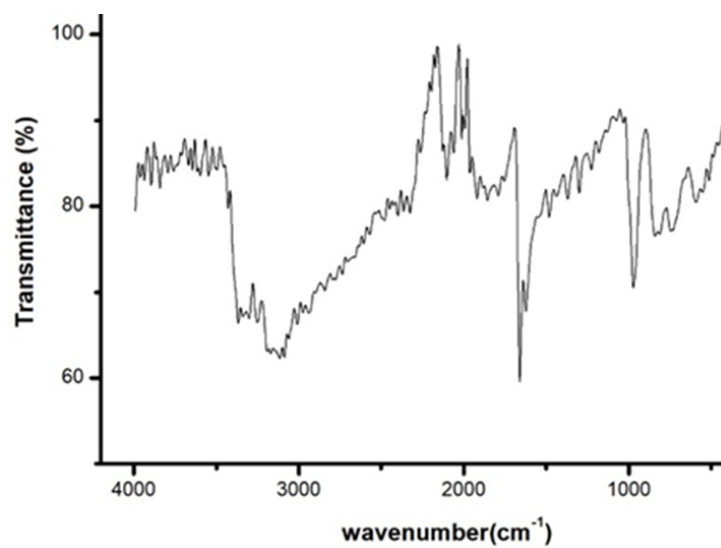


Fig. 5 : FT-IR spectrum of 2A4MPyV10

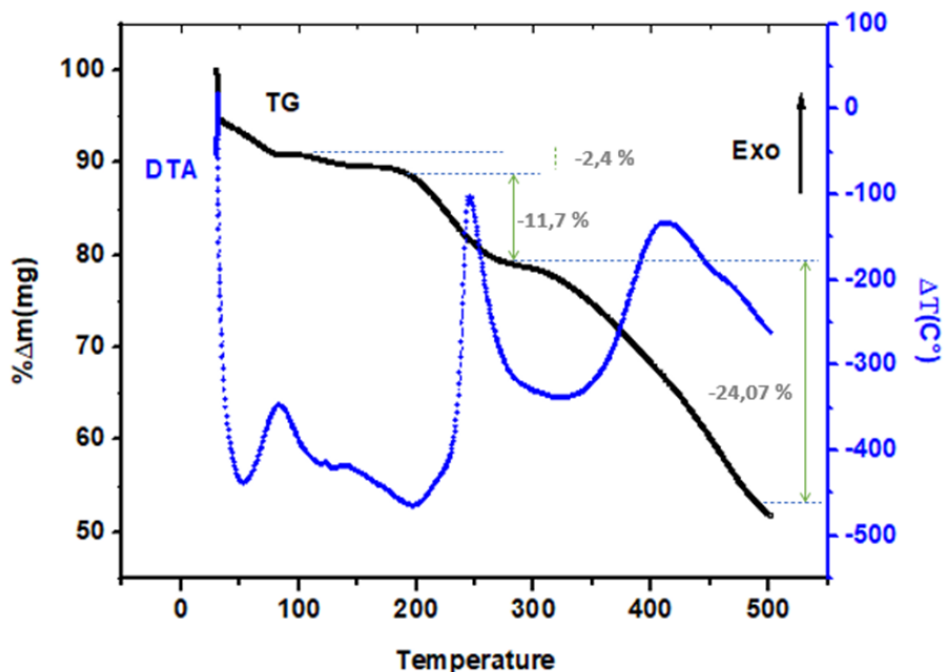


Fig 6: DTA and TGA curves of 2A4MPyV10 at rising temperature.

theoretical mass loss relative to the departure of a molecule of water of crystallization of the compound. The calculated mass loss value is about 2.1%. Subsequently, the dehydrated compound, undergoes a decomposition of its organic and anionic parts in a wide temperature range that starts around 200 °C up to 490 °C and that results in a series of endothermic peaks whose most intense are located around 240 and 430 °C[38]. These phenomena are accompanied by a loss of mass on the TG curve evaluated at 11.76% and 24.07%. This is confirmed by the obtaining of a black carbon residue at the end of the experiment.

4. CONCLUSION

A new synthesized decavanadate adorned with mixed ammonium and organic cations 2A4MPyV10 is reported and characterized. Its crystal structure analysis shows a 3D- supramolecular network of decavanadate ribbons stabilized by $O_{\text{decavanadate}} - H \dots O_{\text{decavanadate}}$ hydrogen bonding interactions. The NH_4^+ and $[2A4MPy - H]^+$ cations and water molecules are located between the ribbons and associated to the decavanadate polyanions through extensive hydrogen bond and Van der Waals interactions. The spectroscopic investigation well evidenced the presence of protonated decavanadate anion and functional groups of organic cations. The thermal analysis indicates that the compound is thermo-stable up to 183°C.

REFERENCES

- [1] T. Duraisamy, N. Ojha, A. Ramanan, J. J. Vittal, *Chem. Mater.* 11 (1999)2339-2349
- [2] Pope, M. T. Muller, A. *Angew. Chem. Int. Ed. Engl.* (1991) 30-34.
- [3] E. Dumas, C. Livage, S. Halut, G. Herve, *Chem. Commun.* (1996) 2437-2438.
- [4] Chen, Q. Zubieta, J. *Coord. Chem. Rev.* (1992)114-107.
- [5] Muller, A. Rohlffing, R. Krickmeyer, E. *Angew. Chem. Int. Ed. Engl.* 32 (1993)909.
- [6] Muller, A. Peters, F. Pope, M. T. Gatteschi, D. *Chem. Rev.* (1998) 98-239.
- [7] J.M. Missina, L.B.P. Leme, K. Postal, F.S. Santana, D.L. Hughes, E.L. de Sá, R.R. Ribeiro, G.G. Nunes, Accessing Decavanadate Chemistry With Tris(hydroxymethyl) Aminomethane, And Evaluation Of Methylene Blue Bleaching, *Polyhedron* 180 (2020) 114414.
- [8] J. Li, C. Wei, D. Guo, C. Wang, Y. Han, G. He, J. Zhang, X. Huang, C. Hu, *J. Name.* (2013)1-3.
- [9] C. Zhang, S. Liu, B. Gao, C. Y. Sun, L. H. Xie, M. Yu, J. Peng, *Polyhedron.* 26 (2007) 1514–1522.
- [10] L.Q. Mai, B. Hu, T. Hu, W. Chen, E.D. Gu, *J. Phys. Chem. B.* 110 (2006) 19083.
- [11] K. Takahashi, Y. Wang, K. Lee, G. Cao, *Appl. Phys. A.* 82 (2006) 27.
- [12] A.M. Evangelou, *Crit. Rev. Oncol. Hematol.* 42 (2002) 249.
- [13] K. Takahashi, S.J. Limmer, Y. Wang, G.Z. Cao, *Japan J. Appl. Phys.* 44 (2005) 662.
- [14] D.W. Boyd, K. Kustin, M. Niwa, *Biochim. Biophys. Acta* 827 (1985) 472.
- [15] E.G. Demaster, R.A. Mitchell, *Biochemistry.* 12 (1973) 3616-3621.
- [16] D.J. Graves, *Biochemistry.* 22 (1983) 4994.

- [17] T. Tiago, M. Paulo, G.M. Carlos, A. Manuel, *Biochim. Biophys. Acta.* 1774 (2007)474
- [18] L. Mai, C. Han, *Mater. Lett.* 62 (2008) 1458.
- [19] E. S. Lara, S.Treviño, B. L. S. Gaytán, E. Sánchez-Mora, M. E. Castro, F. J. Meléndez-Bustamante, M. A. Méndez-Rojas, E. González-Vergara *frontiers in chemistry.* 6(2018) 402.
- [20] L. Mai, C. Han, *Materials Letters.* 62 (2008) 1458–1461.
- [21] L. J. Farrugia, WINGX, A MS-Windows System of Programs for Solving, Refining and Analysing Single Crystal X-ray Diffraction Data for Small Molecules (University of Glasgow, Glasgow, 2005).
- [22] I. D. Brown, M. O’Keefe, A. Navrotsky, *Structure and Bonding in Crystals*, Academic Press, New York.(1981) 1-30.
- [23] G. M. Sheldrick, *Acta Cryst.* 64 (2008)112-122.
- [24] D. Kobashi, S. Kohara, J. Yamakawa, A. Kawahara, *Acta Crystallogr.* 53(1997) 1523.
- [25] S. Toumi, N.R. Ramond, S. Akriche, *J. Clust. Sci.* 26 (2015) 1821.
- [26] J.L. Ferreira da Silva, M.F.M. Piedade, M.T. Duarte, *Inorg. Chim. Acta* 356 (2003) 222.
- [27] A. Durif, M.T. Averbuch-Pouchot, J.C. Guitel, *Acta Crystallogr. B.* 36 (1980) 680.
- [28] J.M. Arrieta, *Polyhedron* 11 (1992) 3045.
- [29] A.S.J. Wery, J.M. Gutierrez-Zorrilla, A. Luque, P. Roman, *Polyhedron* 15 (1996)4555.
- [30] G. Maciejewska, M. Nosek, T. Glowiak, J. Starosta, M. Cieslak-Golonka, *Polyhedron* 22 (2003) 1415.
- [31] R. L. Frost, K. L. Erickson, M. L. Weier, O. Carmody, *Spectrochim. Acta A.* 61 (2005) 829.
- [32] G. Z. Kaziev, A. V. Oreshkina, S. H. Quinones, A. F. Stepnova, V. E. Zavodnik, A. de Ita, D.A. Alekseev, *Russ. J. Coord. Chem.* 36 (2010) 887.
- [33] V. N. Krasil’nikov, A. P. Shtin, L. A. Perelyaeva, I. V. Baklanova, A. P. Tyutyunnik, V. G. Zubkov, *Russ. J. Coord. Chem* 5 (2010) 162.
- [34] L. Klistincova, E. Rakovsky, P. Schwendt *Transit Met. Chem.* 35 (2010) 229.
- [35] A. S. J. Wery, J. M. Gutierrez-Zorrilla, A. Luque, P. Roman, M. Martinez-Ripoll, *Polyhedron.* 15 (1996) 4555.
- [36] P. Roman, A. Aranzabe, A. Luque, J. M. Gutierrez-Zorrilla, M. Martinez-Ripoll, *J Chem Soc Dalton Trans.* (1995) 2225.
- [37] M. Louati, R. Ksiksi, L. J. Jouffret, M. F. Zid, *M.F.CSTA.* 8(2019) 1-11.
- [38] R. Ksiksi, T. Aissa, M. Faouzi, *J. Mol. Struc.*, (2022) 133064.